

Communication

Pyranine Immobilized on Aminopropyl-Modified Mesoporous Silica Film for Paraquat Detection

Sudarat Sombatsri ¹, Krittanun Deekamwong ¹, Pongtanawat Khemthong ² and Sanchai Prayoonpokarach ^{1,*}

¹ School of Chemistry, Institute of Science, Suranaree University of Technology, 111, University Avenue, Nakhon Ratchasima 30000, Thailand

² National Science and Technology Development Agency (NSTDA), National Nanotechnology Center (NANOTEC), Pathum Thani 12120, Thailand

* Correspondence: sanchaip@g.sut.ac.th

Abstract: An optical sensor based on pyranine immobilized on aminopropyl-modified mesoporous silica films was developed for paraquat detection in aqueous solutions. An electrochemically assisted self-assembly method was used to deposit mesoporous silica film on fluorine-doped tin oxide glass. The obtained films were modified with various concentrations of 3-aminopropyl triethoxysilane (APTES) before the immobilization of pyranine. Cyclic voltammetry, scanning electron microscopy, transmission electron microscopy, Fourier transform infrared spectroscopy, and fluorescence spectroscopy were used to characterize the films. Pyranine-immobilized films gave an emission at 506 nm with an excitation at 450 nm. The fluorescence signal was quenched in the presence of paraquat. The films modified with 3% APTES provided the optimum response to paraquat. The developed films had a linear response to paraquat in the concentration range of 1 to 10 ppm at the optimum conditions, with a detection limit of 0.80 ppm. The developed method was used to quantify paraquat in sugarcane peel and tap water samples with satisfactory results.

Keywords: mesoporous silica film; paraquat; pyranine; fluorescence



Citation: Sombatsri, S.;

Deekamwong, K.; Khemthong, P.;

Prayoonpokarach, S. Pyranine

Immobilized on

Aminopropyl-Modified Mesoporous Silica Film for Paraquat Detection.

Chemosensors **2023**, *11*, 249.

<https://doi.org/10.3390/chemosensors11040249>

Academic Editor: Francesco Baldini

Received: 13 March 2023

Revised: 6 April 2023

Accepted: 13 April 2023

Published: 17 April 2023



Copyright: © 2023 by the authors. Licensee MDPI, Basel, Switzerland. This article is an open access article distributed under the terms and conditions of the Creative Commons Attribution (CC BY) license (<https://creativecommons.org/licenses/by/4.0/>).

1. Introduction

Paraquat (PQ) is an herbicide for eliminating unwanted broadleaf weeds [1]. Although the long half-life of PQ causes many human health problems, it is still widely used in many countries in both agricultural and non-agricultural areas due to its relatively high efficiency and low cost. The toxicity of PQ is associated with the reduction of a cationic form (PQ²⁺) to a free radical (PQ^{•+}), which can generate reactive oxygen species (ROS) in the presence of oxygen molecules [2]. These ROSs are well known to damage cell membranes, proteins, and DNA [3]. Moreover, depending on its concentration, ingestion of it into the human body can cause the failure of several organs, such as the liver, kidney, or lung [4]. The Thai Agriculture Standard (TAS 9002-2008) recommends a maximum residue limit (MRL) of 0.05 mg/kg of PQ in fruits and vegetables, which is similar to the Food and Agriculture Organization of the United Nations (FAO) and the World Health Organization (WHO). To track PQ residue efficiently and precisely, easy-to-use sensing methods must be developed.

Many analytical methods for the detection of PQ have been reported. These include gas chromatography–mass spectrometry [5], high performance liquid chromatography [6], and electrochemistry [7], among others. The techniques provide good selectivity and sensitivity and could be adopted for PQ analysis, depending on situations, instruments availability, and skilled operators. Consequently, alternative methods for PQ detection to meet specific needs are being researched and developed.

Recently, a fluorescence method for PQ detection based on the interaction between 8-hydroxypyrene-1,3,6-trisulfonate or pyranine and PQ in aqueous solutions was reported [8]. The interactions between the two species quenched the fluorescence signal from pyranine in aqueous solutions [9]. Although the method was sensitive and selective to PQ, the pyranine

solution was used and discarded after the reaction. The immobilization of pyranine on a solid support could increase the reagent's reusability and decrease waste generation.

Pyranine (Pyr) has been immobilized on solid supports such as ethyl cellulose [10], poly(dimethyl siloxane) combined with poly(2-hydroxyethyl acrylate) [11], and organo-silica sol-gel membranes [12]. However, the immobilized materials were mainly applied as optical pH sensors. The hydroxyl group of Pyr is sensitive to pH change and responsible for the change in fluorescence signal based on an excited-state proton transfer process. The fluorescence intensity depends on the number of protonated/deprotonated forms in different pH levels [13]. The solid supports are not porous, but they allow the diffusion of H^+ through the membranes. There are no reports of Pyr immobilized on porous solid supports as sensors for PQ. Therefore, this work investigated the immobilization of Pyr on a modified mesoporous silica film for the detection of paraquat. The support was a porous material with a pore size of ~ 3 nm, large enough to accommodate the molecules of Pyr and PQ. It was also physically and chemically stable in aqueous solutions.

Mesoporous silica films (MSFs) have attracted considerable attention as solid-support materials due to their unique features, including high specific surface area, silanol surface capable of chemical modification, and high water stability [14]. Such properties are appropriate for immobilizing sensing agents. Among various synthetic methods, the electrochemically assisted self-assembly (EASA) method was able to generate MSFs with vertically oriented mesopore channels on indium tin oxide (ITO) glass [15]. The obtained films were homogenous with a uniform thickness of <150 nm and optically transparent, making them suitable for optical sensor applications. In this work, a PQ sensor based on Pyr immobilized on aminofunctionalized MSFs was developed. MSFs were synthesized on fluorine-doped tin oxide (FTO) glass using the EASA method. The films were modified with aminopropyl silane and immobilized with Pyr. Factors affecting the immobilization of Pyr, including the amount of aminopropyl silane, pH, and time, were investigated. The developed sensor was used to detect PQ, and the sensing parameters and practical utility of the sensor were investigated.

2. Materials and Methods

2.1. Chemical and Reagents

The chemicals used in this work were tetraethyl orthosilicate ($SiC_8H_{20}O_4$, TEOS, 98%, Sigma-Aldrich, Darmstadt, Germany), hexadecyltrimethylammonium bromide ($C_{19}H_{42}BrN$, CTAB, 99%, ACRÖS), 3-aminopropyl triethoxysilane ($C_9H_{23}NO_3Si$, APTES, 99%, ACRÖS, Morris Plains, NJ, USA), ethyl alcohol (C_2H_5OH , 99.9%, Carlo Erba, Val de Reuil, France), sodium nitrate ($NaNO_3$, 99%, Carlo Erba, Val de Reuil, France), hydrochloric acid (HCl, 37%, RCI Labscan, Bangkok, Thailand), hexaammineruthenium (III) chloride ($Ru(NH_3)_6Cl_3$, 99%, Strem Chemicals, Newburyport, MA, USA), potassium hexacyanoferrate (III) ($K_3Fe(CN)_6$, 99%, Merck, Darmstadt, Germany), acetone (CH_3COCH_3 , 99.8%, Carlo Erba, Val de Reuil, France), sodium dihydrogen phosphate anhydrous (NaH_2PO_4 , 99%, QR&C, Auckland, New Zealand), disodium hydrogen phosphate anhydrous (Na_2HPO_4 , 99%, QR&C, Auckland, New Zealand), 8-hydroxypyrene-1,3,6-trisulfonic acid trisodium salt ($C_{16}H_7Na_3O_{10}S_3$, pyranine, 96%, Sigma-Aldrich, Darmstadt, Germany), and methyl viologen hydrate ($C_{12}H_{14}N_3$, paraquat, 98%, ACRÖS, Morris Plains, NJ, USA). Deionized (DI) water was used to prepare all aqueous solutions.

2.2. Synthesis of MSFs on FTO Glass

MSFs were deposited on FTO glass (OPV tech, surface resistivity 7–8 Ω /sq) using the EASA method [15]. A sol consisting of 20 mL of ethanol, 20 mL of 0.1 M $NaNO_3$, 13.6 mmol of TEOS, and 4.35 mmol of CTAB (CTAB/TEOS ratio = 0.32) was prepared by stirring. Before use, the pH of the sol solution was adjusted to 3 with 0.1 M HCl and aged for 2.5 h under stirring. The FTO glass was ultrasonically cleaned in a detergent solution, DI water, ethanol, and acetone for 15 min in each liquid. The cleaned FTO glass was immersed in the prepared sol mixture, and a cathodic potential of -1.3 V was applied for 60 s. The

resultant FTO glass was quickly removed from the solution, rinsed with DI water, and dried overnight at 130 °C. To create empty channels of mesoporous silica, CTAB was extracted using an ethanol solution containing 0.1 M HCl.

2.3. Modification of MSFs with APTES

The MSFs were modified using a postgrafting method according to the literature [16]. MSFs were immersed in an ethanol solution containing APTES for 24 h at 60 °C under refluxed conditions. After that, the films were washed with acetone and ethanol and dried at 80 °C for 2 h to give aminopropyl-modified MSFs (NH₂-MSFs). The concentration of APTES used in the modification step was varied between 1, 3, and 5% (v/v).

2.4. Immobilization of Pyranine

NH₂-MSFs were immersed in 0.1 M HCl for 1 h under stirring and rinsed with DI water to protonate amino groups in the films. Pyr was immobilized by soaking the films in a 1.0 mM Pyr solution. The immobilization time and pH of the solutions were varied to obtain an optimum amount of Pyr in the films. The Pyr-immobilized films were rinsed with DI water and dried at room temperature for 24 h.

2.5. Paraquat Response to Sensing Film

The response of PQ to the sensing films was investigated using fluorescence spectroscopy. A sensing film was immersed in an ethanol–buffer solution containing paraquat. Fluorescence spectra were taken at an emission wavelength of 506 nm and an excitation wavelength of 450 nm. The response of the sensing films to foreign species was optimized by immersing the sensing films in a PQ solution and a PQ solution mixed with foreign species such as K⁺, Cu²⁺, Zn²⁺, Fe³⁺, and carbaryl.

2.6. Analysis of Real Samples

The developed sensing films were used to detect the concentrations of PQ in tap water and sugarcane peel samples. Sugarcane samples were collected from sugarcane fields in Nong Ruea, Khon Kaen Province, Thailand. Tap water samples were collected from Suranaree University of Technology, Nakhon Ratchasima, Thailand. The PQ extraction procedure described in the literature [17,18] was used for the sugarcane peel samples. Sugarcane peel weighing 25.0 g was added to 100 mL of methanol mixed with 0.1 M HCl (1:1 v/v). The mixture was refluxed at 80 °C for 15 min. After cooling to room temperature, the liquid phase was separated by filtration through No.1 Whatman paper, adjusted to pH 6 with NaOH, and then diluted to the volume of 200 mL with DI water. Finally, 5.00 mL of the resultant liquid was treated with 0.50 mL of 5% EDTA and made up to 10 mL with phosphate buffer. For tap water samples, the analysis of PQ was conducted with a suitable pH adjustment of the samples.

2.7. Characterization

All electrochemical measurements were carried out with a potentiostat (EMStat3+, PalmSens, Houten, The Netherlands). The permeability and continuity of the films were evaluated with cyclic voltammetric experiments using a Pt plate (1 × 1 cm²) as a counter electrode, Ag/AgCl as a reference electrode, and FTO glass as a working electrode in 0.1 M NaNO₃ solution as an electrolyte. Ru(NH₃)₆³⁺ and Fe(CN)₆³⁻ were used as electroactive probes. Cyclic voltammograms were recorded at 0.1 Vs⁻¹ for 5 scans. Film morphology was investigated by a scanning electron microscope (SEM, JSM-6010LV, JEOL, Tokyo, Japan) and a transmission electron microscope (TEM, Talos F200X, Thermo Fisher Scientific, Branchburg, NJ, USA). Functional groups on the films were identified with a Fourier transform infrared spectrometer (FTIR, Tensor27-Hyperion, Bruker, Billerica, MA, USA). Fluorescence signal measurements were performed on a fluorescence spectrophotometer (LS 50 B, Perkin Elmer, Waltham, MA, USA).

3. Results and Discussion

3.1. Characterization of MSF

The EASA method was used to synthesize ordered mesoporous silica films attached to FTO glass. The film was hexagonally packed with mesopore channels, as can be seen in the TEM images in Figure 1a,b. Some silica particles were found on the top surface, as seen in the SEM image in Figure 1c. Figure 1d shows an SEM image of a cross-section of the film with a thickness of ~170 nm.

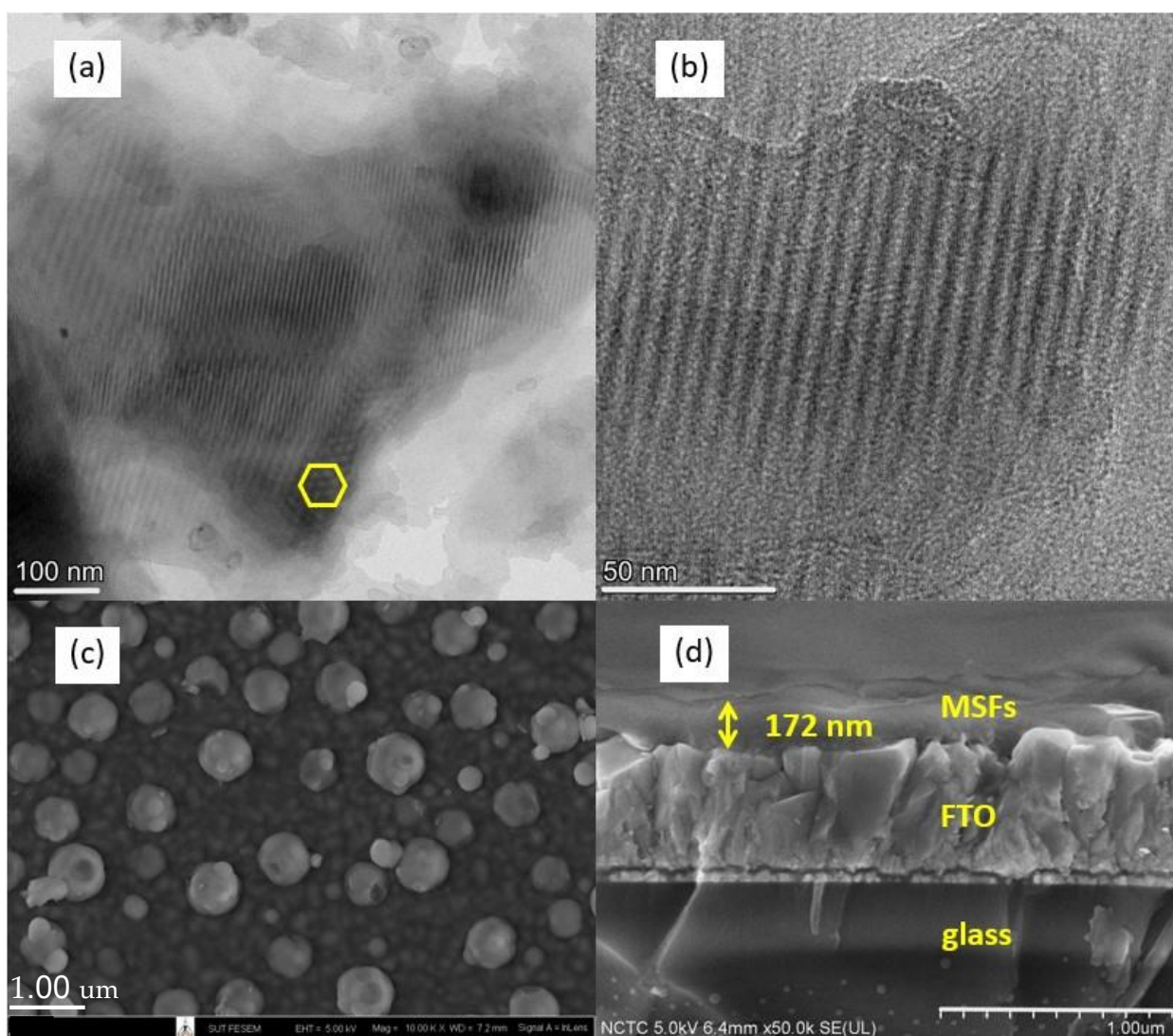


Figure 1. TEM images of mesoporous silica film stripped from the substrate (a,b). SEM images of the film on FTO glass, top view (c), and cross-sectional view (d).

The accessibility of the pore channels was investigated with cyclic voltammetry (CV) using $\text{Ru}(\text{NH}_3)_6^{3+}$ and $\text{Fe}(\text{CN})_6^{3-}$ as redox probes. Figure 2a shows that no redox signal of $\text{Ru}(\text{NH}_3)_6^{3+}$ was observed on the as-prepared film because the pores were filled with CTAB. This indicates that the film was deposited over the FTO glass without cracks. After CTAB was removed from the film, the redox probe could access the electrode surface resulting in the observed signals. There was no redox reaction at the electrode surface when $\text{Fe}(\text{CN})_6^{3-}$ was used as a probe, as shown in Figure 2b. According to the findings, the surface of the pores had a negative polarity [16], which prevented the anionic probe from diffusing to the electrode surface. Therefore, to immobilize Pyr, which has three sulfonic groups, the surface of the pores should be modified.

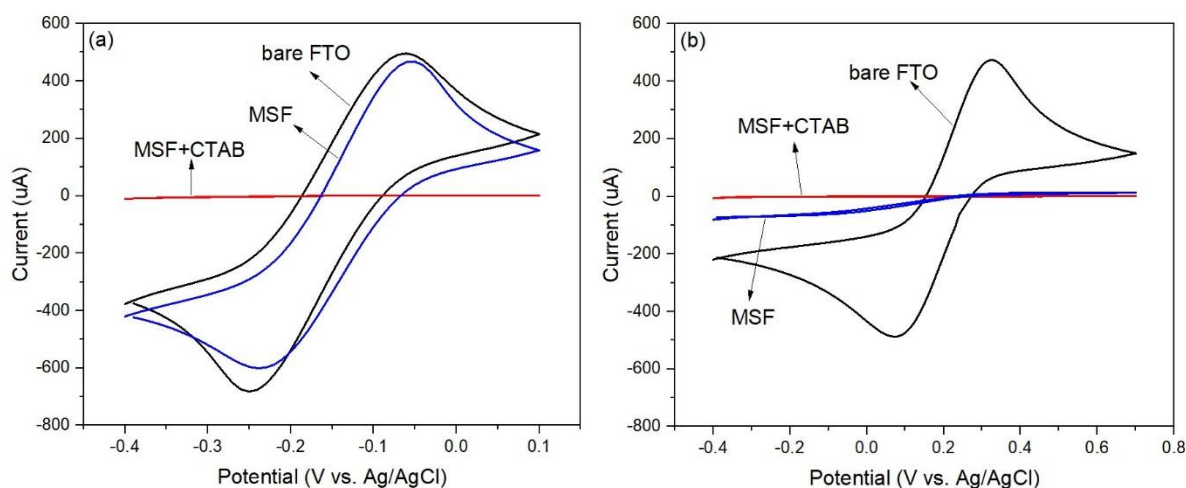


Figure 2. Cyclic voltammograms of MSFs before/after surfactant removal were recorded in 0.1 M NaNO_3 solution containing 5 mM $\text{Ru}(\text{NH}_3)_6^{3+}$ (a) and 5 mM $\text{Fe}(\text{CN})_6^{3-}$ (b) at a scan rate of 0.1 Vs^{-1} .

3.2. Characterization of Aminopropyl-Modified MSFs

FTIR was used to confirm functional groups grafted on the MSFs. The spectra are shown in Figure 3. The band at 1066 cm^{-1} is associated with the Si-O-Si stretching. The bands at 2977 cm^{-1} and 2893 cm^{-1} are related to the C-H stretching of aminopropyl. The peaks at 1520 cm^{-1} and 1398 cm^{-1} are ascribed to $-\text{NH}_2$ bending and C-N stretching, respectively. The observed bands were in similar regions as those reported in the study of APTES functionalized onto porous silicon [19], mesoporous silica [20], and SBA-15 silica [21]. It was also observed that the peak intensity at 1520 cm^{-1} increased with an increase in the APTES concentration used in the silica surface modification. The results indicated that APTES was successfully incorporated on the surface of MSFs.

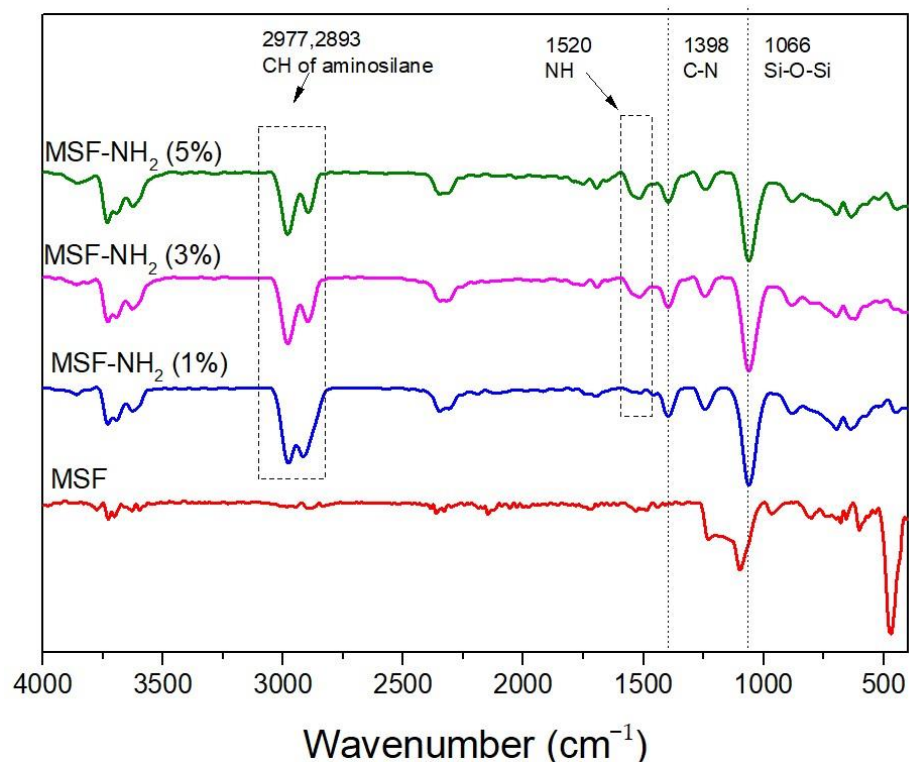


Figure 3. FTIR spectra of aminopropyl-modified MSFs and MSF on FTO glass.

Cyclic voltammetry was used to investigate the MSFs after modification with APTES. The modified films were soaked in an acidic solution to protonate the -NH_2 groups before placing them in a probe solution. The results are shown in Figure 4. The signals from the modified films were lower than those from the unmodified film, as shown in Figure 4a. The lower signals could be from charge repulsion between the probe species, $\text{Ru}(\text{NH}_3)_6^{3+}$, and the protonated aminopropyl. In addition, the signals for the films modified with a higher concentration of APTES decreased. More aminopropyl groups could make the pores less permeable to the probe species.

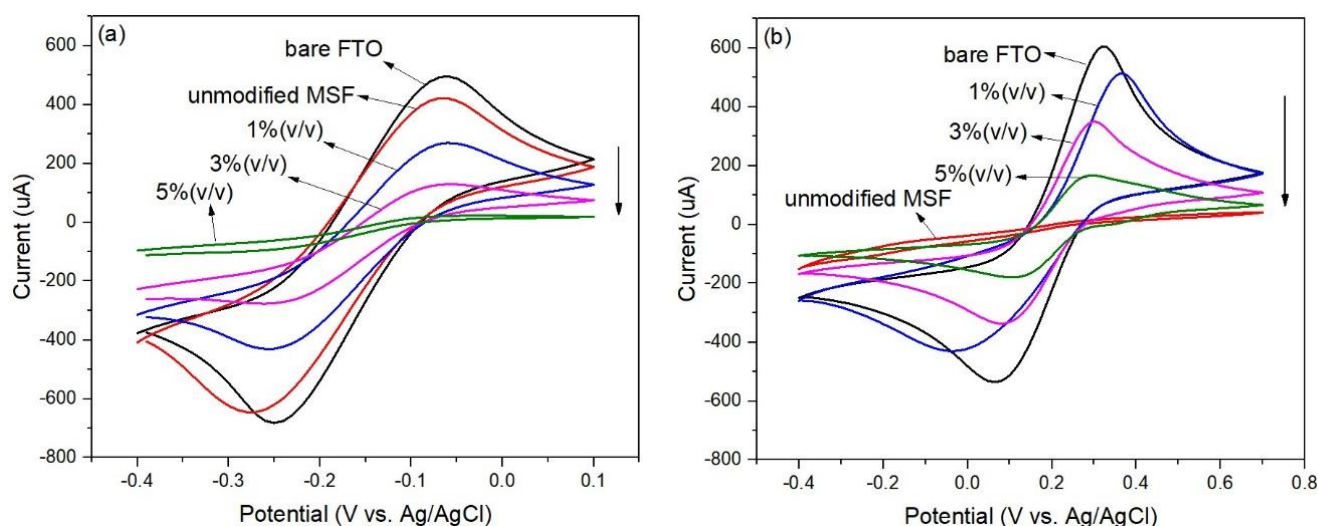


Figure 4. Cyclic voltammograms of MSFs modified with various concentrations of APTES in 0.1 M NaNO_3 solution containing 5 mM $\text{Ru}(\text{NH}_3)_6^{3+}$ (a) and 5 mM $\text{Fe}(\text{CN})_6^{3-}$ (b) at scan rate of 0.1 Vs^{-1} .

Figure 4b shows that the unmodified MSF gave no signal when tested with the anionic redox probe, $\text{Fe}(\text{CN})_6^{3-}$. However, the modified films showed signal responses to the probe species indicating that the presence of protonated aminopropyl assisted the diffusion to the electrode surface. In addition, the signals for the films modified with a higher concentration of APTES decreased. More aminopropyl groups could hinder the diffusion of the probe species to the electrode surface.

3.3. Immobilization and Optimization of Sensing Films

Pyr was immobilized by immersing the modified MSFs in a 1.0 mM Pyr solution. Figure 5 shows a Pyr-immobilized film, which is light yellow. The film had an emission peak at 506 nm when excited at 450 nm.

The MSFs were immobilized with Pyr after being modified with different concentrations of APTES, and the results are shown in Figure 6. The fluorescence intensity at 506 nm at pH 6.0 increased with an increase in the APTES concentration, indicating that more Pyr was immobilized. It was also observed that as the APTES concentration increased, the color of the Pyr became more intense. The 5%-APTES-modified MSF had the highest fluorescence intensity and was off-scale. Pyr was also found to be slightly leached into the solution. As a result, the MSF modified with 3% APTES was chosen for further investigation. In addition, no fluorescence peak of Pyr was observed for the unmodified MSF. The result supported the negative polarity of the pore channels, which repelled the anionic Pyr. Ionic interaction between the sulfonic groups of Pyr and the protonated aminopropyl on the silica surface could be the primary force responsible for dye immobilization.

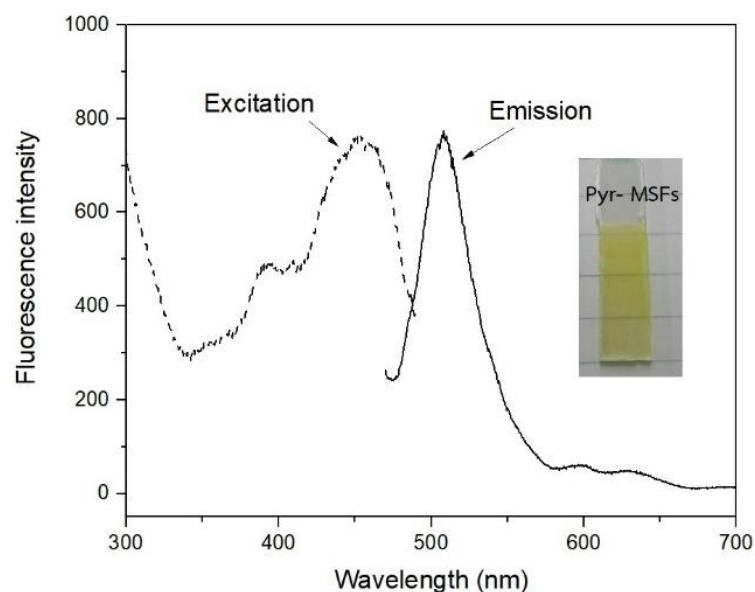


Figure 5. A picture and fluorescence spectra of Pyr immobilized on modified MSF.

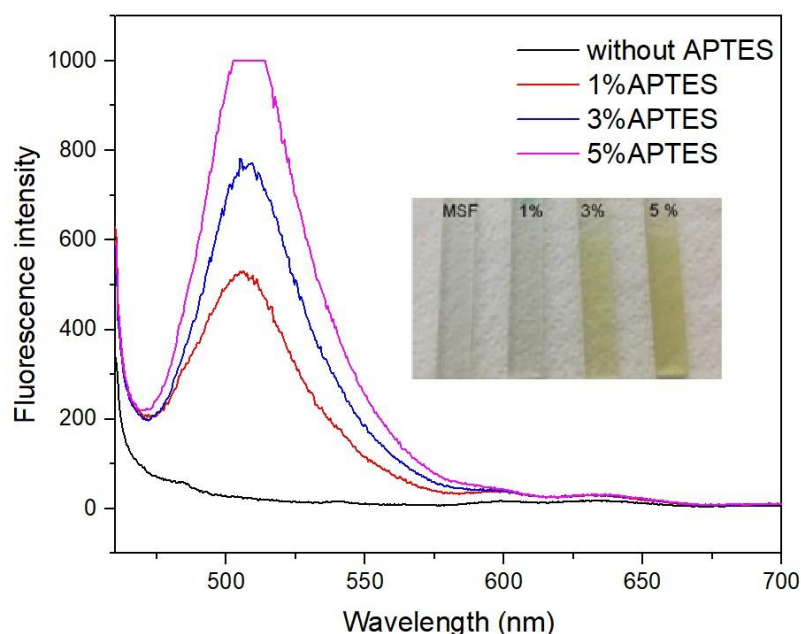


Figure 6. Fluorescence spectra of sensing films with different concentrations of APTES at pH 6.0.

To optimize the fluorescence signal obtained from the films, Pyr was immobilized on MSFs modified with 3% APTES for 1, 6, 12, and 24 h. As shown in Figure 7a, the fluorescence intensity increased with an increase in the soaking time. The best signal was obtained from the film with a 24-h soaking period, which was further used for the immobilization step. The amount of Pyr on the film was estimated to be 1.75×10^{-4} mmol.

The effect of pH on the fluorescence signal of the Pyr-immobilized MSFs was investigated in the pH range of 4.0–7.0. After 30 min of soaking in phosphate buffers, the fluorescence spectra of Pyr-immobilized MSFs were recorded, and the results are shown in Figure 7b. The fluorescence intensity increased with an increase in the pH. More deprotonation of the OH group on Pyr could result in the deprotonated Pyr species fluorescing at ~ 506 nm when the pH of the solutions is raised from 4.0 to 7.0 [22]. The maximum intensity was achieved at pH 7.0. Lower pH values could cause the hydrogen ions in the solution to interact with the sulfonic groups of Pyr, producing lower anionic Pyr species to interact with the film. Even though the maximum signal was obtained at pH 7.0, the dye leached

slightly from the sensing film into the solution. Because there was no significant leaching at pH 6.0, the pH of the sample solutions was kept at this level in the subsequent study.

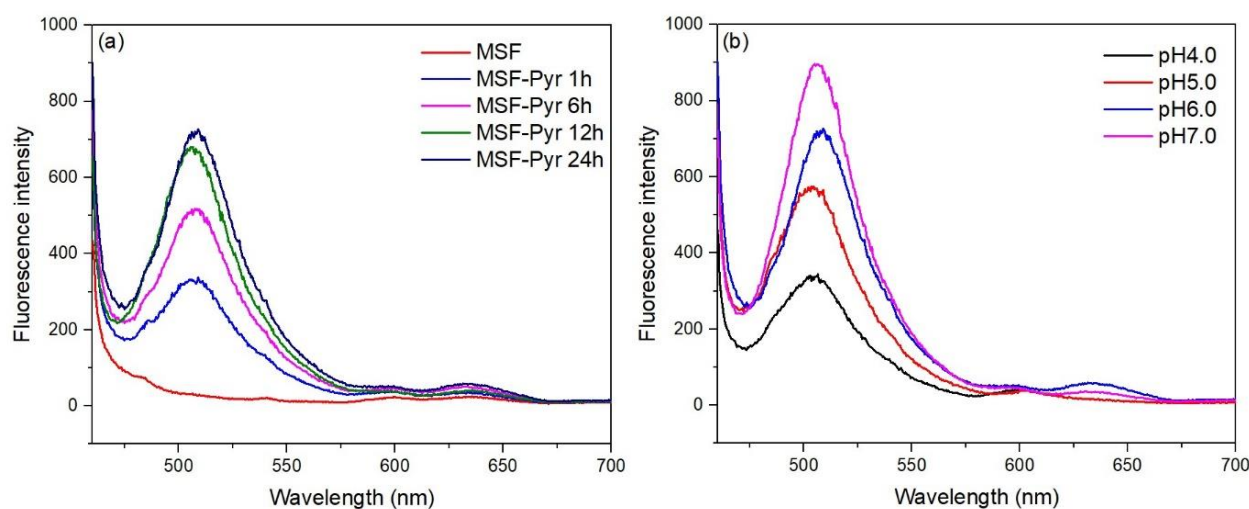


Figure 7. (a) Effect of time on dye immobilization at pH 6.0. (b) Effect of pH of solution on film condition.

The reproducibility of the sensing film fabrication procedure was investigated by measuring the fluorescence intensity of sensing films prepared from ten batches of synthesized gel mixtures, each comprising five films. The fluorescence signals are shown in Figure 8. The calculated relative standard deviation of the signals obtained from each batch was less than 3.0%, while the value was 7.1% for all batches combined. These results confirmed that the fabrication procedure was reproducible.

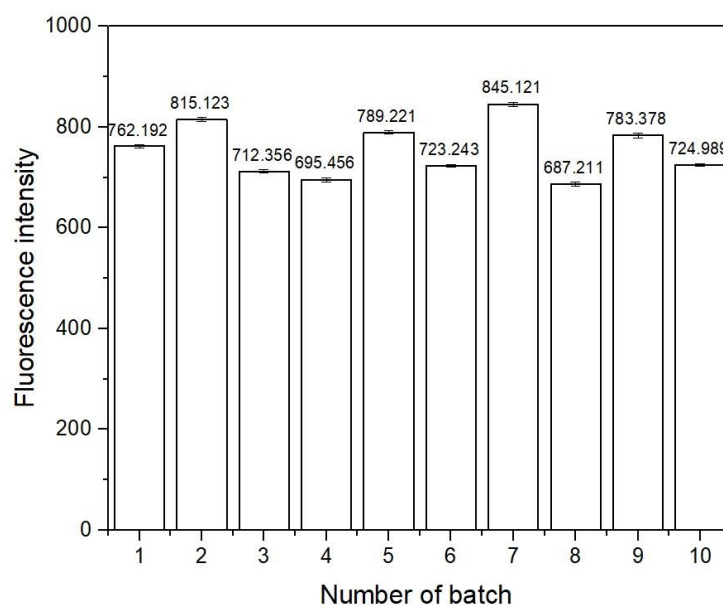


Figure 8. Fluorescence intensity of sensing films from different batches at 506 nm.

3.4. Response of Sensing Film to PQ

The response of Pyr-MSFs to PQ was investigated. A Pyr-MSF was immersed in a buffer solution of pH 6.0 for 10 min, and the fluorescence signal was recorded at 506 nm. The obtained signal was denoted as I_0 . The sensing film was then immersed in a 10 mL PQ solution buffered at pH 6.0 for 5 min. The recorded fluorescence signal was denoted as I . As illustrated in Figure 9a, the fluorescence intensity decreased with an increase in PQ concentration.

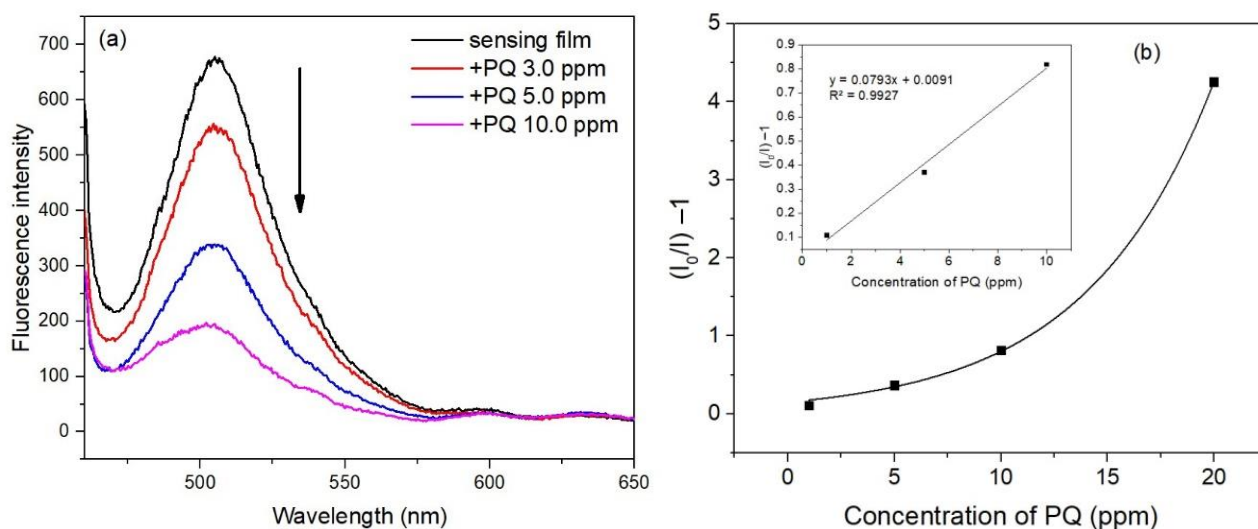


Figure 9. Responses of the sensing film to PQ (a) and a Stern–Volmer plot for PQ quenching of sensing films, inset: a linear relationship in the concentration range 1–10 ppm (b).

The fluorescence intensity decrease could be from the formation of a charge transfer complex between Pyr and PQ, where Pyr acted as an electron donor and PQ acted as an electron acceptor [8,9]. Photoexcitation of Pyr causes the dissociation of the proton from the hydroxyl group of Pyr generating Pyr cation radical and electron. PQ accepts the electron resulting in the photo inactive complex [9]. The fluorescence quenching of Pyr by PQ can be expressed by the Stern–Volmer Equation (1),

$$I_0/I = 1 + K_{SV}[PQ] \quad (1)$$

where I_0 is the fluorescence intensity of the sensing film after soaking in a buffer with pH 6.0 for 10 min, and I is the fluorescence intensity of the film after immersion in a PQ solution. K_{SV} is the Stern–Volmer constant, and $[PQ]$ is the concentration of PQ. A Stern–Volmer plot of $I_0/I - 1$ versus PQ concentration is shown in Figure 9b where a linear relationship was obtained in the concentration range of 1–10 ppm.

The linear correlation coefficient (R^2) was 0.9927. The limit of detection (LOD) was calculated to be 0.80 ppm using Equation (2),

$$\text{LOD} = 3s_{bk}/m \quad (2)$$

where s_{bk} is the standard deviation of the blank measurements and m is the slope of the Stern–Volmer plot.

3.5. Reproducibility and Regeneration

The reproducibility of the sensing films' responses to PQ was assessed by monitoring the fluorescence signals of five sensing films in a 5.0 ppm PQ solution at 506 nm for 5 min. The results clearly showed that the films responded to PQ in a reproducible manner, with a relative standard deviation of 4.4%. In addition, three sensing films were assessed for their responses in a series of PQ solutions at 3.0, 5.0, and 10.0 ppm. The results are shown in Figure 10. The signals received from each film at the same PQ concentration were about the same. The relative standard deviations were 0.9, 3.7, and 3.0% for 3.0, 5.0, and 10.0 ppm PQ solutions, respectively.

The regeneration of a sensing film was studied. After exposure to a 10.0 ppm PQ solution, one sensing film was placed in a 0.01 M phosphate buffer of pH 7.0 to remove PQ. Figure 11 shows that the initial signal of the film dropped slightly after the first regeneration. A similar pattern was observed in the subsequent regeneration cycles. The I/I_0 ratios of the first three replicate measurements using the same sensing film yielded

a relative standard deviation of 5.3%. However, four replicate measurements yielded a higher relative standard deviation of 7.8%. The finding indicated that the film could be reused three times for consistent results. The decrease in initial fluorescence intensity could be due to the incomplete removal of PQ from the sensing film and the leaching of Pyr. The leaching of Pyr can also affect the stability of the sensing film, limiting its repetitive use.

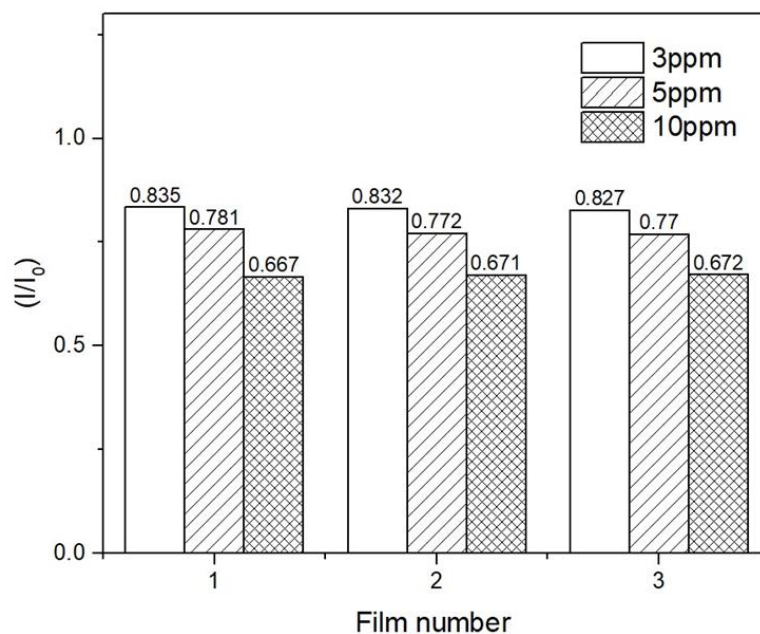


Figure 10. The recycling process for one sensing film.

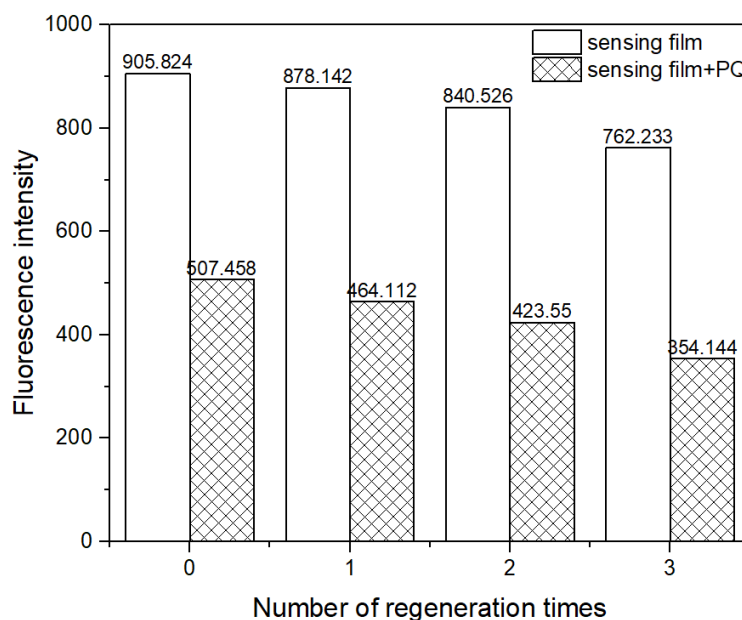


Figure 11. Regeneration of the sensing film.

3.6. Effect of Foreign Species

The effect of foreign species (Cu^{2+} , Fe^{2+} , Zn^{2+} , K^+ , and carbaryl) on the response of the sensing films to PQ was evaluated. The species selected for the study were based on their capabilities to complex with Pyr and the possibility of their presence in samples where the samplings were made. The measurements were taken by recording the fluorescence signal of the sensing films in PQ solutions with and without the tested species. The molar ratio of PQ to the tested species was 1:5, with a fixed PQ concentration of 3.90×10^{-5} M.

Table 1 summarizes the findings. None of the tested species resulted in a change in the sensor response to PQ, as the error was <1.4%.

Table 1. Effect of foreign species.

| Tested Species | % Error * |
|------------------|-----------|
| Cu ²⁺ | 1.08 |
| Fe ²⁺ | 0.53 |
| Zn ²⁺ | 1.34 |
| K ⁺ | 0.31 |
| Carbaryl | 0.55 |

* %Error = $100 \times (I_{r, PQ/tested\ species} - I_{r, PQ}) / I_{r, PQ}$, where I_r is the quenching fraction defined as $(I_0 - I) / I_0$, $I_{r, PQ/tested\ species}$ is the quenching fraction of the film in a PQ solution in the presence of the tested species, and $I_{r, PQ}$ is the quenching fraction of the film in a PQ solution without the tested species.

The applicability of the developed sensor was demonstrated through the measurement of PQ in real samples. PQ was not found in the samples of sugarcane peel or tap water when measured. Furthermore, the samples were spiked with a PQ standard solution, and the results are presented in Table 2. The obtained recoveries and relative standard deviations indicated the suitable reliability of the developed method for measuring PQ in water and sugarcane peel samples. The developed method in this work is compared to other reported optical methods in Table 3. The present work has a linear range and detection limit among those reported in the literature. Immobilizing the sensing reagent on a solid support provides a simple manipulation of the sensor and the potential for recycling the material.

Table 2. Determination of PQ in tap water and sugarcane peel samples.

| Sample | PQ Added (ppm) | PQ Found (ppm) ^a | %Recovery | %RSD |
|----------------|----------------|-----------------------------|-----------|------|
| Tap water | 0 | ND ^b | - | - |
| Tap water | 10.0 | 9.90 ± 0.16 | 99.0 | 1.6 |
| Sugarcane peel | 0 | ND | - | - |
| Sugarcane peel | 10.0 | 10.10 ± 0.51 | 101.0 | 5.0 |

^a The reported values were the average ± standard deviation ($n = 3$). ^b ND = not detected.

Table 3. Different methods used for detection of PQ.

| Sensor Material | Detection Technique | Linear Range (μM) | Limit of Detection (μM) | Reference |
|--|--|---------------------------|-------------------------|-----------|
| Imidacloprid stabilized silver nanoparticles | Colorimetry | 20–180 | 6.3 | [23] |
| Gold nanoparticles modified with 3-mercaptopropylsulfonate | Colorimetry | 0.004–1.9 | 0.004 | [24] |
| Citrate coated AgNPs | Colorimetry | 0.2–194 | 0.19 | [25] |
| Nitrogen doped graphene quantum dots/Hg ²⁺ | Fluorescence | 0.2–7.8 | 0.074 | [26] |
| CdSe/ZnS quantum dots | Fluorescence (quenching) | 3.8×10^{-5} –0.2 | 0.012 | [27] |
| Squaraine | Fluorescence | 0–140 | 0.372 | [28] |
| Ascorbic acid in basic medium | Colorimetry (multisyringe flow injection analysis) | 0.02–1.0 | 0.003 | [29] |
| Pyr-APTES-MSF | Fluorescence (quenching) | 3.9–39 | 3.5 | this work |

4. Conclusions

An optical chemical sensor based on pyranine immobilized on aminopropyl-modified MSFs for paraquat detection was successfully developed. The EASA technique provided

a fast synthesis of ordered mesoporous structured MSFs on FTO glass. The films were modified with aminopropyl silane before the immobilization of pyranine. The developed sensor was simple to use and could be incorporated into a conventional setup spectrometer for fluorometric measurements. The sensor contained a small amount of the reagent and could be reused several times with good reproducibility and reliability. Although the detection limit of the developed method was 0.80 ppm, the method could be used to screen samples with paraquat contamination at concentrations > 1 ppm with a short analysis time of about 5 min/sample.

Author Contributions: Conceptualization, S.S. and S.P.; methodology, S.S. and S.P.; validation, S.S. and S.P.; formal analysis, S.S. and S.P.; investigation, S.S., K.D. and S.P.; data curation, S.S.; writing-original draft preparation, S.S. and S.P.; writing-review and editing, S.S., K.D., P.K. and S.P.; visualization, S.S., K.D. and S.P.; validation, S.S. and S.P.; supervision, S.P.; project administration, S.S. and S.P.; funding acquisition, S.P. All authors have read and agreed to the published version of the manuscript.

Funding: This work was supported by (i) Suranaree University of Technology (SUT), (ii) Thailand Science Research and Innovation (TSRI), and (iii) National Science, Research and Innovation Fund (NSRF) (NRIIS No.160349).

Institutional Review Board Statement: Not applicable.

Informed Consent Statement: Not applicable.

Data Availability Statement: Not applicable.

Acknowledgments: This work was supported by (i) Suranaree University of Technology (SUT), (ii) Thailand Science Research and Innovation (TSRI), and (iii) National Science, Research and Innovation Fund (NSRF) (NRIIS No.160349). S. Sombatsri acknowledges Rajamangala University of Technology Isan, Thailand, for a Ph.D. scholarship. Thida Ounjaidee and Nichakorn Pornnongsan are acknowledged for their assistance in the synthesis experiments. Martha Maloi Eromine is gracefully acknowledged for language assistance.

Conflicts of Interest: The authors declare no conflict of interest.

References

1. Paraquat Information Centre. Available online: <http://paraquat.com/use> (accessed on 9 February 2023).
2. Bus, J.S.; Aust, S.D.; Gibson, J.E. Paraquat toxicity: Proposed mechanism of action involving lipid peroxidation. *Environ. Health Perspect.* **1976**, *16*, 139–146. [[CrossRef](#)] [[PubMed](#)]
3. Peter, B.; Wartena, M.; Kampinga, H.H.; Konings, A.W. Role of lipid peroxidation and DNA damage in paraquat toxicity and the interaction of paraquat with ionizing radiation. *Biochem. Pharmacol.* **1992**, *43*, 705–715. [[CrossRef](#)]
4. Tsai, W.T. A review on environmental exposure and health risks of herbicide paraquat. *Toxicol. Environ. Chem.* **2013**, *95*, 197–206. [[CrossRef](#)]
5. Gao, L.; Liu, J.; Yuan, H.; Deng, X. Solid-phase microextraction combined with GC-MS for determination of diquat and paraquat residues in water. *Chromatographia* **2015**, *78*, 125–130. [[CrossRef](#)]
6. Sha, O.; Wang, Y.; Chen, X.-B.; Chen, J.; Chen, L. Determination of paraquat in environmental water by ionic liquid-based liquid phase extraction with direct injection for HPLC. *J. Anal. Chem.* **2018**, *73*, 862–868. [[CrossRef](#)]
7. Nasir, T.; Herzog, G.; Hébrant, M.; Despas, C.; Liu, L.; Walcarius, A. Mesoporous silica thin films for improved electrochemical detection of paraquat. *ACS Sens.* **2018**, *3*, 484–493. [[CrossRef](#)]
8. Zhao, Z.; Zhang, F.; Zhang, Z. A facile fluorescent “turn-off” method for sensing paraquat based on pyranine-paraquat interaction. *Spectrochim. Acta A Mol. Biomol. Spectrosc.* **2018**, *199*, 96–101. [[CrossRef](#)]
9. de Borja, E.B.; Amaral, C.L.C.; Politi, M.J.; Villalobos, R.; Baptista, M.S. Photophysical and photochemical properties of pyranine/methyl viologen complexes in solution and supramolecular aggregates a switchable complex. *Langmuir* **2000**, *16*, 5900–5907. [[CrossRef](#)]
10. Hakonen, A.; Hulth, S. A high-precision ratiometric fluorosensor for pH: Implementing time-dependent non-linear calibration protocols for drift compensation. *Anal. Chem. Acta.* **2008**, *606*, 63–71. [[CrossRef](#)]
11. Ulrich, S.; Osypova, A.; Panzarasa, G.; Rossi, R.M.; Bruns, N.; Boesel, L.F. Pyranine-modified amphiphilic polymer conetworks as fluorescent ratiometric pH sensors. *Macromol. Rapid Commun.* **2019**, *40*, 1900360. [[CrossRef](#)]
12. Nivens, D.A.; Schiza, M.V.; Angel, S.M. Multilayer sol-gel membranes for optical sensing applications: Single layer pH and dual layer CO₂ and NH₃ sensors. *Talanta* **2002**, *58*, 543–550. [[CrossRef](#)]

13. Giuliano, K.A.; Gillies, R.J. Determination of intracellular pH of BALB/c-3T3 cells using the fluorescence of pyranine. *Anal. Biochem.* **1987**, *167*, 362–371. [[CrossRef](#)]
14. Innocenzi, P.; Malfatti, L. Mesoporous thin films: Properties and applications. *Chem. Soc. Rev.* **2013**, *42*, 4198–4216. [[CrossRef](#)]
15. Walcarius, A.; Sibottier, E.; Etienne, M.; Ghanbaja, J. Electrochemically assisted self-assembly of mesoporous silica thin films. *Nat. Mater.* **2007**, *6*, 602–608. [[CrossRef](#)] [[PubMed](#)]
16. Ding, L.; Li, W.; Sun, Q.; He, Y.; Su, B. Gold nanoparticles confined in vertically aligned silica nanochannels and their electrocatalytic activity toward ascorbic acid. *Chem. Eur. J.* **2014**, *20*, 12777–12780. [[CrossRef](#)] [[PubMed](#)]
17. Kolberg, D.I.S.; Mack, D.; Anastassiades, M.; Hetmanski, M.T.; Fussell, R.J.; Meijer, T.; Mol, H.G.J. Development and independent laboratory validation of a simple method for the determination of paraquat and diquat in potato, cereals and pulses. *Anal. Bioanal. Chem.* **2012**, *404*, 2465–2474. [[CrossRef](#)]
18. Pizzutti, T.R.; Vela, G.M.E.; Kok, A.; Scholten, J.M.; Dias, J.V.; Cardoso, C.D.; Concenço, G.; Vivian, R. Determination of paraquat and diquat: LC-MS method optimization and validation. *Food Chem.* **2016**, *209*, 248–255. [[CrossRef](#)]
19. Majoul, N.; Aouida, S.; Bessaïs, B. Progress of porous silicon APTES functionalization by FTIR investigations. *Appl. Surf. Sci.* **2015**, *331*, 388–391. [[CrossRef](#)]
20. Farook, A.; Kasim, H.M.; Hasnah, O. Synthesis of mesoporous silica immobilized with 3-[(mercapto or amino)propyl]trialkoxysilane by a simple one-pot reaction. *Chin. J. Chem.* **2010**, *28*, 2383–2388.
21. Ribeiro, J.O.N.; Nunes, E.H.M.; Vasconcelos, D.C.L.; Vasconcelos, W.L.; Nascimento, J.F.; Grava, W.M.; Derks, P.W.J. Role of the type of grafting solvent and its removal process on APTES functionalization onto SBA-15 silica for CO₂ adsorption. *J. Porous Mater.* **2019**, *26*, 1581–1591. [[CrossRef](#)]
22. Hong, Y.; Cheong, B.; Cho, H. Excited-state proton transfer reaction of pyranine in aqueous sugar and alcohol solutions investigated by fluorescence spectroscopy. *Bull. Korean Chem. Soc.* **2017**, *38*, 1333–1339. [[CrossRef](#)]
23. Ali, S.; Shah, M.R.; Hussain, S.; Khan, S.; Latif, A.; Ahmad, M.; Ali, M. A facile approach based on functionalized silver nanoparticles as a chemosensor for the detection of paraquat. *J. Clust. Sci.* **2022**, *33*, 413–420. [[CrossRef](#)]
24. Zhang, Y.; Huang, Y.; Fu, L.; Qiu, J.; Wang, Z.; Wu, A. Colorimetric detection of paraquat in aqueous and fruit juice samples based on functionalized gold nanoparticles. *J. Food. Compost. Anal.* **2020**, *92*, 103574. [[CrossRef](#)]
25. Siangproh, W.; Somboonsuk, T.; Chailapakul, O.; Songsrirote, K. Novel colorimetric assay for paraquat detection on-silica bead using negatively charged silver nanoparticles. *Talanta* **2017**, *174*, 448–453. [[CrossRef](#)] [[PubMed](#)]
26. Du, F.; Sun, L.; Zen, Q.; Tan, W.; Chaen, Z.; Ruan, G.; Li, J. A highly sensitive and selective “on-off-on” fluorescent sensor based on nitrogen doped graphene quantum dots for the detection of Hg²⁺ and paraquat. *Sens. Actuators B Chem.* **2019**, *288*, 96–103. [[CrossRef](#)]
27. Durán, G.M.; Contento, A.M.; Ríos, A. Use of CdSe/ZnS quantum dots for sensitive detection and quantification of paraquat in water samples. *Anal. Chim. Acta.* **2013**, *801*, 84–90. [[CrossRef](#)]
28. Tu, J.; Xiao, L.; Jiang, Y.; He, Q.; Sun, S.; Xu, Y. Near-infrared fluorescent turn-on detection of paraquat using an assembly of squaraine and surfactants. *Sens. Actuators B Chem.* **2015**, *215*, 382–387. [[CrossRef](#)]
29. Maya, F.; Estels, J.M.; Cerdà, V. Improved spectrophotometric determination of paraquat in drinking waters exploiting a multisyringe liquid core waveguide system. *Talanta* **2011**, *85*, 588–595. [[CrossRef](#)]

Disclaimer/Publisher’s Note: The statements, opinions and data contained in all publications are solely those of the individual author(s) and contributor(s) and not of MDPI and/or the editor(s). MDPI and/or the editor(s) disclaim responsibility for any injury to people or property resulting from any ideas, methods, instructions or products referred to in the content.